Research and Applications in Structural Engineering, Mechanics and Computation – Zingoni (Ed.)
© 2013 Taylor & Francis Group, London, ISBN 978-1-138-00061-2

The impact of fire scenario to the collapse of a tall structure

S. Selamet
Bogazici University, Istanbul, Turkey

ABSTRACT: The aim of this study is to investigate the effect of the fire load to a tall structure and draw conclusions for a more robust structural design. If a building is not properly designed and constructed to withstand potentially catastrophic events due to risk factors posed by fires, such disasters can nullify the benefits gained from green construction. Leadership in Energy and Environmental Design (LEED) developed by the U.S. Green Building Council and other international certification organizations. One common aspect of most of these certification systems is a lack of consideration for the impact of risks such as fire hazard on sustainability. In order to design sustainable tall structures, their robustness against extreme fire scenarios must be adequately satisfied. In this study, a generic tall structure is modeled using the finite element software LS-Dyna. The two-dimensional model consists of line elements (beams and columns) as well as the shell elements (concrete deck). To simulate the building collapse, the explicit dynamic analysis is used with proper surface-based contact configurations.

1 INTRODUCTION

The progressive collapse behavior of tall buildings has been intensively studied after the collapse of World Trade Center Towers in 2001 (Hoffman, 2004, Gross, 2005). A sensitivity analysis of a moment resisting and a dual system steel frame due to a column loss is conducted by Kim et al. (2011) and they concluded that the beam yield strength is the most critical design parameter. A detailed three-dimensional composite floor structure with shear connections is modeled by Sadek et al. (2008) and Alashker et al. (2010). One-floor composite structure is suddenly subjected to a column loss and it is observed that the tensile forces in the composite floor are carried by the metal deck. Further, the effect of shear connection capacity is found to be limited. A similar observation is made by Yu et al. (2009). A comprehensive three-dimensional model of the eight-story Cardington steel frame building is created by Kwasniewski (2010). The nonlinear dynamic behavior is analyzed due to column loss at different locations and due to increased gravity loading. The dynamic behavior of a 20 story steel building is investigated due to column loss with several different column locations by Fu (2009). Izzuddin et al. (2008) and Vlassis et al. (2009) laid out a theoretical groundwork for steel frames due to a sudden column loss. A steel building might also collapse due to an extreme event such as fire. The underlying mechanisms of tall buildings when subjected to fire have been previously investigated by Lange et al. (2012). It was found that the main cause of collapse is the outward and inward deflection of the columns above and below the heated floor. These columns are called as ‘pivot columns’. Sun et al. (2012) investigated the vulnerability of steel braced frames and the development of plastic hinges at elevated temperatures.

In light of the described previous research on this subject, the main objective of this study is the assessment of the structural response of a 49 story steel high-rise structure due to ISO834 fire. It is intended to provide a better understanding of the effect of fire loading leading to the collapse mechanism of a high-rise structure. For all case studies, 3 floors are heated simultaneously at different floor locations and regions (asymmetric vs. symmetric heating). The commercial finite element code LS-Dyna is used as the analysis tool for the uncoupled thermo-mechanical dynamic response of the structure. Simulations are carried out using the Central Difference explicit time integration scheme. Geometric nonlinearity in terms of large displacements and rotations are taken into account. Material nonlinear response is considered through the use of a bi-linear constitutive model. The steel yield stress and stiffness of the material vary at elevated temperatures according to Eurocode provisions. The high-rise steel frame consists of steel beams and columns modeled with 2-node 1D (line) finite elements and composite floors modeled with 4-node shell 2D finite elements. In order to cut down the computational expense, the beam and columns are not modeled with shell elements, which could have accurately captured the local buckling effects during fire as discussed by Selamet & Garlock (2012). The structural load carrying system of the high-rise structure is assumed to be a moment resisting frame. Perimeter (primary) beams are connected to each other and to columns with rigid (moment) connections, the secondary beams and the bracing members have pinned connections.

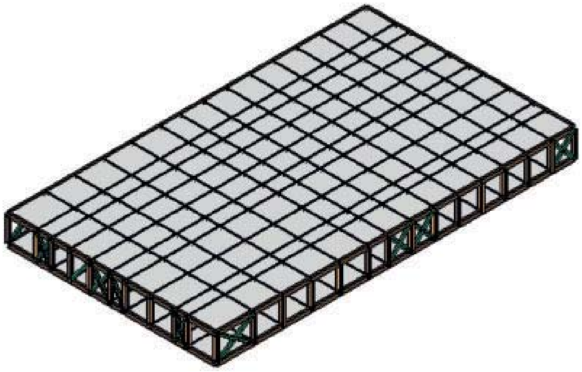

Figure 1. The floor structure of the tall building model.

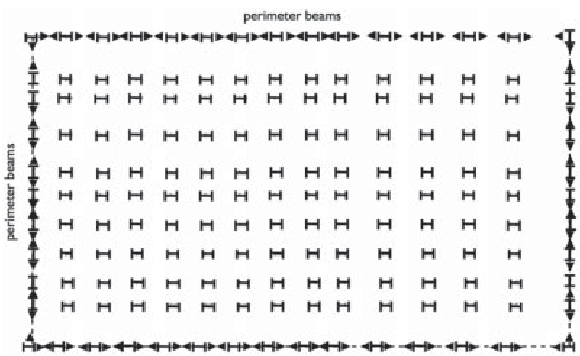

Figure 2. The column orientations for moment frame design.

2 TALL BUILDING STRUCTURE

2.1 *Design*

The tall steel structure is first modeled in ETABS, widely used structural engineering software. The steel frame sections (i.e. primary and secondary beams, bracings and columns) are designed with a combined earthquake and gravity load according to ASCE\SEI 7-10 seismic loading provisions (ASCE 2010). The prototype composite floor layout is based on Chase Tower (formerly known as BankOne) in Chicago, IL and it consists of secondary beams, primary beams, lateral bracings and 10 cm thick concrete slab with full composite action with the secondary beams. The building has 50 m by 29 m floors with a total height of 179 m. The model deflection calculations takes account the contribution of the concrete slab to the flexural stiffness; however this contribution is neglected for steel design calculations as a conservative approach. The height of each floor is 3.6 m and the member size of the columns is decreased at every 10th floor. Figure 1 and Figure 2 show the extruded view of a typical steel floor and the column orientations, respectively. The beam member sizes are shown in Table 1. The connections between the primary and secondary beams are idealized as pinned connections and the perimeter (primary) beams are connected with moment connections as part of the moment frame design. The bracings are modeled as truss elements. The prototype composite floor shown in Figure 1 is replicated for the upper floors.

Table 1. The structural steel member sizes.

Structural member	Steel section
Primary beam	W24 × 146
Secondary beam	W14 × 34
Lateral bracings	W14 × 120
Column (1–10th)	W24 × 335
Column (11–20th)	W24 × 306
Column (21–30th)	W24 × 207
Column (31–40th)	W24 × 146
Column (41–49th)	W24 × 103

2.2 *Gravity and earthquake loads for design*

The dead load is assumed to be the self-weight of the steel members and the superimposed dead load, which is estimated to be 3.6 kN/m^2. The superimposed dead load includes the weight of the light-weight concrete and the other structural elements such as partitions. The live load is assumed to be 2.4 kN/m^2, which is typical for an office building according to ASCE 7-10. The steel members are assumed to carry the gravity load depending on their tributary areas. The first natural period of the tall building is calculated as $T_d = 2.6174$ sec. Both the modal response spectrum analysis and the equivalent lateral force analysis methods are used for the earthquake design. Los Angeles CA region is taken as a basis for both methods. The response modification R and the occupancy importance I factors are taken as 8 and 3, respectively. The 0.2 sec (S_s) and the 1.0 sec (S_1) spectral accelerations are found as 2.1226 sec and 0.7837 sec, respectively. The base shear coefficient is calculated by ETABS as $C_w = 0.177$.

3 FINITE ELEMENT MODEL IN LS-DYNA

3.1 *Model description*

The geometry of the entire tall building model in ETABS is imported to LS-Dyna for uncoupled thermo-mechanical analysis with various fire scenarios, which requires an explicit dynamic scheme with highly nonlinear material behavior as well as large displacements. The Hughes-Liu beam elements and Belytschko-Tsay shell elements are employed in the model. The shell elements only provide additional stiffness to the building as a diaphragm. A rigid body is placed on the base to provide contact surface for the collapsed floors as seen in Figure 3. The gravity loading defined in the design is applied by using *LOAD BODY Z command for 6 seconds to ensure that no significant inertial (dynamic) forces are created before the fire starts. The reactions due to dead and live loads at the base are validated with the ETABS results. In order to simulate

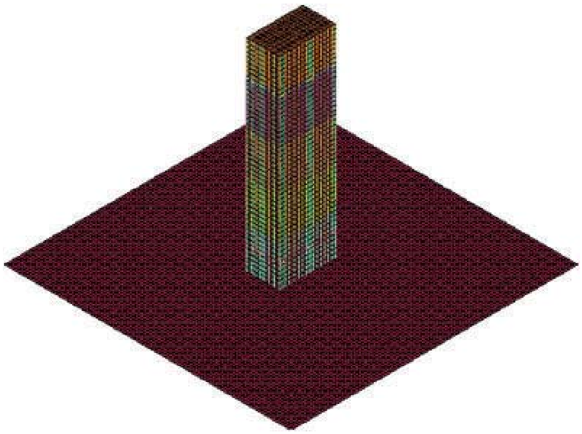

Figure 3. The tall building model in LS-Dyna with rigid base.

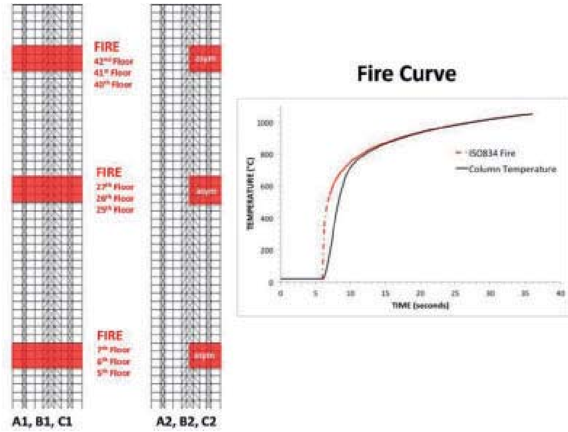

Figure 4. The fire location and progression in the tall building.

Table 2. Temperature dependent properties of steel.

T (°C)	20	100	300	500	600	700	900	1100
ρ (kg/m^3)	7850	7850	7850	7850	7850	7850	7850	7850
E (GPa)	200	200	160	120	62	26	13.5	4.5
σ_y (MPa)	345	345	345	269	162	79	21	4.3
ν	0.3	0.3	0.3	0.3	0.3	0.3	0.3	0.3
E_t/E	0.01	0.01	0.01	0.01	0.01	0.01	0.01	0.11
$\alpha(\times 10^{-5})$ (1/°C)	1.23	1.25	1.33	1.41	1.45	1.49	1.34	1.46

Table 3. Properties of the concrete slab.

ρ (kg/m^3)	E (GPa)	σ_y (MPa)	ν –	E$_t$ (GPa)	Failure strain –
1750	24.8	27.6	0.2	24.8×10^{-2}	0.05

progressive collapse, the contact interactions are introduced between the shells, beams and the rigid surface with *CONTACT GENERAL command. The steel material in the heated floors is defined as temperature dependent with *MAT ELASTIC PLASTIC THERMAL command. This material type does not have a failure limit state. Due to this limitation, the steel material for the other (not heated) floors is defined as temperature independent with *MAT PIECEWISE LINEAR PLASTICITY.

The temperature dependent material strength and stiffness of the steel sections and the material properties of the concrete slab are given in Table 2. A simple bilinear stress-strain relationship (constant E_t) is assumed, which is based on Eurocode 3 (CEN 2001). Since the concrete is not heated in the model, only ambient temperature material properties are used as seen in Table 2. For simplicity, no reinforcement bars are modeled for the concrete material. The temperature dependent thermal expansion coefficient α of steel is taken from Eurocode 3.

Table 4. Fire scenarios.

Label	Floor location	Fire spread
Case A1	5th–7th	Symmetrical
Case B1	25th–27th	Symmetrical
Case C1	40th–42nd	Symmetrical
Case A2	5th–7th	Asymmetrical
Case B2 25th–27th	Asymmetrical	
Case C2 40th–42nd	Asymmetrical	

3.2 *Gravity loading and fire scenarios*

A total of 6 fire scenarios are investigated, which are illustrated in Figure 4 and defined in Table 4. In conducting these scenarios, the aim is to understand the effect of the fire location (bottom, middle or top floors) and the fire spread (symmetric or asymmetric). For all cases, the steel building is gradually (quasi-statically) loaded with the dead load and the live load for 6 seconds. No oscillations are observed during the gravity loading, which validates that the loading remained static. The unprotected column members are heated with ISO834 fire curve as seen in Figure 4 (CEN 2001). The fire curve is applied at 6 seconds soon after the gravity load is applied. For computational efficiency, the fire curve is scaled to range only to 36 seconds as shown in Figure 4. Within the period, the kinetic energy of the system is carefully monitored in order to get a quasi-static behavior of the building during the thermal loading. The steel temperatures are calculated using lumped mass method with four-sided heating with convective heat transfer coefficient $h = 25$ W/m^2°C and emissivity $\varepsilon = 0.5$. No fire protection is applied to the columns. ISO834 fire curve and the lumped column temperature are shown in Figure 4. The temperatures are directly applied to the nodes without a heat transfer analysis in LS-Dyna (uncoupled thermo-mechanical analysis). For Cases A through C, three columns at 5th–6th–7th floors, 25th–26th–27th floors and 40th–41st–42nd floors are heated uniformly considering a symmetrical collapse (A1, B1

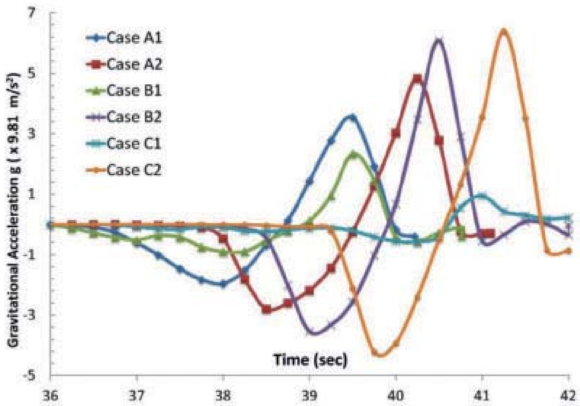

Figure 5. Rigid body acceleration of the entire building in the vertical direction.

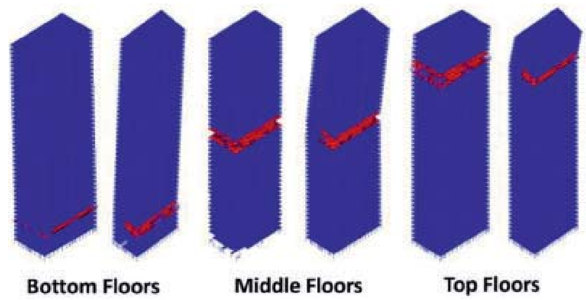

Figure 6. The collapse initiation for all cases. The heated floors are in red (lighter color).

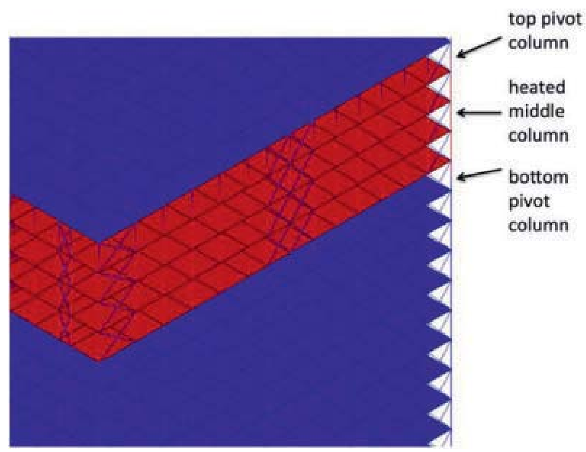

Figure 7. The location of the heated and pivot corner columns in the tall building for all cases.

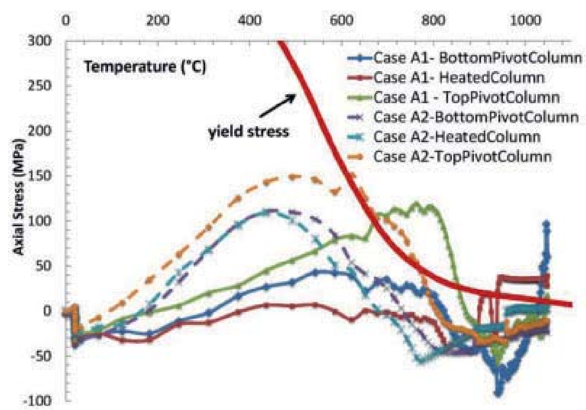

Figure 8. Column axial stress-temperature history for bottom floors fire (Cases A1 and A2).

and C1), respectively. For Cases 4 through 6, only half of the regions at 5th–6th–7th floors, 25th–26th–27th floors and 40th–41st–42nd floors are heated (A2, B2 and C2), respectively. Hence, the asymmetrical collapse is expected. After the plastic deformations of the structural members in the fire-applied floor, the gravity loading is scaled 5 times until 40 seconds to initiate collapse.

4 OBSERVATION AND RESULTS

4.1 *Collapse characteristics*

Figure 5 clearly shows the distinct collapse characteristics of the tall steel building. The collapse initiates soon after the fire application is over at around 36 seconds. At the onset of the collapse, the building has downward (negative) acceleration in g-units. But as the collapse progresses, the acceleration reserves the sign as the lower floors resist the impact and the downward motion slows down. The severity of the collapse is larger for the asymmetric fires. In general a fire in the lower floors causes the collapse initiation to occur slightly earlier. Further, the asymmetric collapse causes the building to lean over to one side and more debris is spread to a larger area on the rigid base as seen in Figure 6. This is a great concern in urban areas with high density of tall buildings in the neighboring regions. It is also observed that the asymmetric collapse in the lower floors causes an overturning moment, which tears apart the base columns and the shell elements in the cool (not heated) region.

4.2 *Column axial forces*

To analyze the behavior of the tall building at the collapse instant, the axial stress development of the three corner columns observed as shown in Figure 7. The heated column is compared to the (pivot) columns right below and above the heated region. Figures 8 through 10 show the axial stress development in these columns for Cases A, B and C, respectively.

In addition, the temperature dependent yield stress capacity of the columns is plotted. Note for some pivot columns, the axial stress surpasses the yield stress at some instances, which is expected since these pivot columns stay at ambient temperature. As seen in Figure 8, the initial compressive (negative) stress in the column due to gravity is considerably low. This is expected since the model is specially designed for lateral (earthquake) resistance of a large earthquake. It is observed that the heated column carries a minimum load whereas the pivot columns go into tensile action to the outward movement of the floors due to expansion.

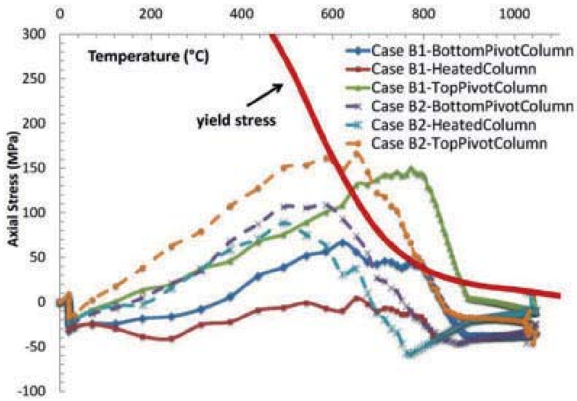

Figure 9. Column axial stress-temperature history for middle floors fire (Cases B1 and B2).

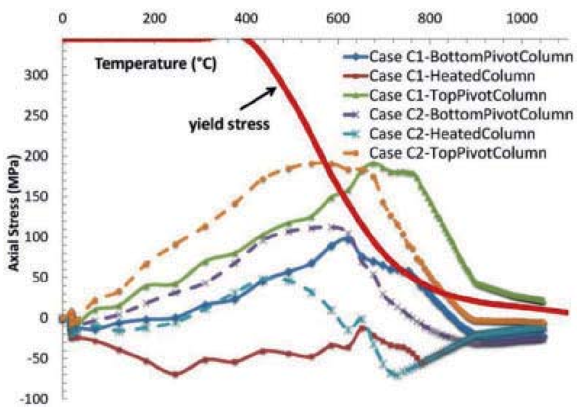

Figure 10. Column axial stress-temperature history for top floors fire (Cases C1 and C2).

The top pivot column carries the maximum load until it fails first at around 800°C. The difference between the symmetric and asymmetric collapse is seen in the magnitude of these stresses. Further, for the asymmetric case, the sudden drop in column stresses is seen at around 600°C.

Figures 9 and 10 show the same trend but the heated column has larger compression and the pivot columns have larger tension. This can be explained by the visual inspection in Figure 6. In Cases C1 and C2 with the heated top floors, the building leans over towards the corner region more than the other cases, which causes the stresses to differ significantly larger between the pivot and heated columns.

5 CONCLUSION

This study presents the ongoing research on the collapse mechanisms of tall steel buildings with symmetric and asymmetric fire conditions and various fire floor locations. The observations suggest that the asymmetric heating causes the steel building to collapse by leaning on the side that corresponds to the heated floor region. It also suggests that a building designed even for a large earthquake is not resistant to weakened floors due to the imposed ISO834 fire. In general, an asymmetric fire spread causes more damage to the building and the building collapse initiates earlier when compared to a symmetrical fire spread. The fire location seems to change the collapse behavior only slightly. In all cases, the pivot columns below and above the heated regions go into tension due to the lateral expansion of the floors. The author intends to expand the study by adding the *MAT EROSION command for the heated steel members. Furthermore, a finer meshing in the beam members will enable to capture a possible buckling behavior.

ACKNOWLEDGEMENTS

This research is funded by Bogazici University Scientific Research Project (BAP) No. 7122: 13A04P1. All opinions, findings and conclusions expressed in this paper are the authors' and do not necessarily reflect the policies and views of BAP.

REFERENCES

Alashker, Y., El-Tawil, S., Sadek, F. 2010. Progressive collapse resistance of steel-concrete composite floors. *Journal of Structural Engineering ASCE* 136 (10): 1187–1196.

ASCE 2010. ASCE/SEI 7-10 Minimum Design Loads for Buildings and Other Structures (1st Edition). Reston: Virginia.

CEN 2001. Eurocode 3: Design of steel structures Part 1.2: General Rules Structural fire design ENV 1993-1-2:2001. Brussels: Belgium.

Fu, F. 2009. Progressive collapse analysis of high-rise building with 3-D finite element modeling method. *Journal of Constructional Steel Research* 65: 1269–1278.

Gross, J.L. & McAllister, T.P. 2005. Structural fire response and probable collapse sequence of the World Trade Center Towers. Federal building and fire safety investigation of the World Trade Center disaster (NIST NCSTAR 1-6), *NIST*. Gaithersburg: Maryland.

Hoffmann, C., Popescu, V., Kilic, S.A., Sozen, M. 2004. Modeling, simulation, and visualization: The Pentagon on September 11th. *Computing in Science & Engineering (CISE)* 6(1): 52–60.

Izzuddin, B.A., Vlassis, A.G., Elghazouli, A.Y., Nethercot, D.A. 2009. Progressive collapse of multi-storey buildings due to sudden column loss – Part I: Simplified assessment framework. *Engineering Structures* 30: 1308–1318.

Kim, J., Park, J-H., Lee, T-H. 2011. Sensitivity analysis of steel buildings subjected to column loss. *Engineering Structures* 33: 421–432.

Kwasniewski, L. 2010. Nonlinear dynamic simulations of progressive collapse for a multistory building. *Engineering Structures* 32: 1223–1235.

Lange, D., Roeben, C., Usmani, A. 2012. Tall building collapse mechanisms initiated by fire: Mechanisms and design methodology. *Engineering Structures* 36: 90–103.

LSTC 2012. LS-DYNA Keyword User's Manual Volume I & II version 971. Livermore: California.

Sadek, F., El-Tawil, S., Lew, H.S. 2008. Robustness of composite floor systems with shear connections: Modeling, simulation, and evaluation. *Journal of Structural Engineering ASCE* 134(11): 1717–1725.

Selamet, S., & Garlock, M. 2012. Plate buckling strength of steel wide-flange sections at elevated temperatures. *Journal of Structural Engineering ASCE* doi: 10.1061/(ASCE)ST.1943-541X.0000769.

Sun, R., Huang, Z., Burgess I.W. 2012. The collapse behaviour of braced steel frames exposed to fire. *Journal of Constructional Steel Research* 72: 130–142.

Vlassis, A.G., Izzuddin, B.A., Elghazouli, A.Y., Nethercot, D.A. 2009. Progressive collapse of multi-storey buildings due to failed floor impact. *Engineering Structures* 31: 1552–1534.

Yu, M., Zha, X., Ye, J. 2010. The influence of joints and composite floor slabs on effective tying of steel structures in preventing progressive collapse. *Journal of Constructional Steel Research* 66: 442–451.